Conjugation of Arginine-Glycine-Aspartic Acid Peptides to Poly(ethylene oxide)-*b*-poly(ϵ-caprolactone) Micelles for Enhanced Intracellular Drug Delivery to Metastatic Tumor Cells

Xiao-Bing Xiong,[†] Abdullah Mahmud,[†] Hasan Uludağ,[†,‡] and Afsaneh Lavasanifar*[,†]

Faculty of Pharmacy and Pharmaceutical Sciences and Department of Chemical & Materials Engineering, Faculty of Engineering, University of Alberta, Edmonton, Alberta T6G 2N8, Canada

Received October 6, 2006; Revised Manuscript Received December 6, 2006

An arginine-glycine-aspartic acid (RGD) containing model peptide was conjugated to the surface of poly(ethylene oxide)-*block*-poly(ϵ-caprolactone) (PEO-*b*-PCL) micelles as a ligand that can recognize adhesion molecules overexpressed on the surface of metastatic cancer cells, that is, integrins, and that can enhance the micellar delivery of encapsulated hydrophobic drug into a tumor cell. Toward this goal, PEO-*b*-PCL copolymers bearing acetal groups on the PEO end were synthesized, characterized, and assembled to polymeric micelles. The acetal group on the surface of the PEO-*b*-PCL micelles was converted to reactive aldehyde under acidic condition at room temperature. An RGD-containing linear peptide, GRGDS, was conjugated on the surface of the aldehyde-decorated PEO-*b*-PCL micelles by incubation at room temperature. A hydrophobic fluorescent probe, that is, DiI, was physically loaded in prepared polymeric micelles to imitate hydrophobic drugs loaded in micellar carrier. The cellular uptake of DiI loaded GRGDS-modified micelles by melanoma B16-F10 cells was investigated at 4 and 37 °C by fluorescent spectroscopy and confocal microscopy techniques and was compared to the uptake of DiI loaded valine-PEO-*b*-PCL micelles (as the irrelevant ligand decorated micelles) and free DiI. GRGDS conjugation to polymeric micelles significantly facilitated the cellular uptake of encapsulated hydrophobic DiI most probably by intergrin-mediated cell attachment and endocytosis. The results indicate that acetal-terminated PEO-*b*-PCL micelles are amenable for introducing targeting moieties on the surface of polymeric micelles and that RGD-peptide conjugated PEO-*b*-PCL micelles are promising ligand-targeted carriers for enhanced drug delivery to metastatic tumor cells.

Introduction

New blood vessels formed in a tumor to provide nutrients and oxygen for growing tumor cells usually have large gaps in their endothelium. This allows the extravasation of nanoparticles to the extravascular space surrounding the tumor cells. The permeated nanocarrier usually gets trapped in the tumor because the lymphatic system that drains fluids out of other organs is absent in tumors. This phenomenon, known as the enhanced permeation and retention (EPR) effect, is believed to be the reason for the passive accumulation of carriers of <200 nm with prolonged blood circulation properties (e.g., polymeric micelles and stealth liposomes) in solid tumors.

Polymeric micelles are core/shell structures formed through self-assembly of amphiphilic block copolymers. The nanoscopic dimension as well as unique properties offered by separated core and shell domains of polymeric micelles has made them one of the most promising carriers for drug targeting by EPR in cancer.[1−3] The nanoscopic size of polymeric micelles makes the carrier unrecognizable by the phagocytic cells of the reticuloendothelial system (RES) and prolongs their blood circulation.[4] The small size of polymeric micelles is also expected to facilitate carrier's extravasation from tumor vasculature and to ease the penetration of the extravasated carrier within a solid tumor tissue. Finally, a capacity for the stabilized encapsulation of hydrophobic compounds offered by polymeric micelles is considered as one of their advantages over other colloidal systems for targeted delivery of anticancer agents, most of which are hydrophobic.

Research in the field of polymeric micellar drug delivery has been expanded tremendously during the past decade. However, achieving high targeting efficiency for hydrophobic drugs by polymeric micelles at the tumor site still remains a major challenge. Despite high accumulation of nanosized micelles in tumor tissue as a result of EPR effect, accumulation of the encapsulated drug at the cellular and molecular drug targets cannot be guaranteed.[5−7] Efficient drug targeting by polymeric micelles in most cases is hampered by either premature drug release from the micellar nanocontainers before the carrier reaches the tumor targets or insufficient intracellular delivery of the encapsulated anticancer drug to the tumor cells.[6] Finding the right polymeric micellar system that can provide a proper balance between the two properties, that is, avoiding premature drug release outside tumor site but promoting cellular internalization or obtaining triggered drug release at the tumor site, poses a challenge for efficient targeted drug delivery by polymeric micelles.

Several studies suggest that attachment of cell-specific ligands on the surface of colloidal carriers can be used as an efficient strategy to enhance cellular internalization of nanocarriers at desired tissue.[8−11] In this context, covalent attachment of cell-specific ligands, for example, sugars, peptides, and monoclonal antibodies, on the surface of polymeric micellar delivery systems has been pursued to enhance drug delivery to various cells.[12−15] For tumor targeting, cancer-specific peptides are more appropriate than monoclonal antibodies because they are smaller and

* To whom correspondence should be addressed. Phone: 780-492-2742. Fax: 780-492-1217. E-mail: alavasanifar@pharmacy.ualberta.ca.
[†] Faculty of Pharmacy and Pharmaceutical Sciences.
[‡] Department of Chemical & Materials Engineering.

10.1021/bm060967g CCC: $37.00
Published on Web 02/22/2007

Scheme 1. Synthetic Scheme and Models for the Preparation of DiI Encapsulated GRGDS-PEO-*b*-PCL Micelles

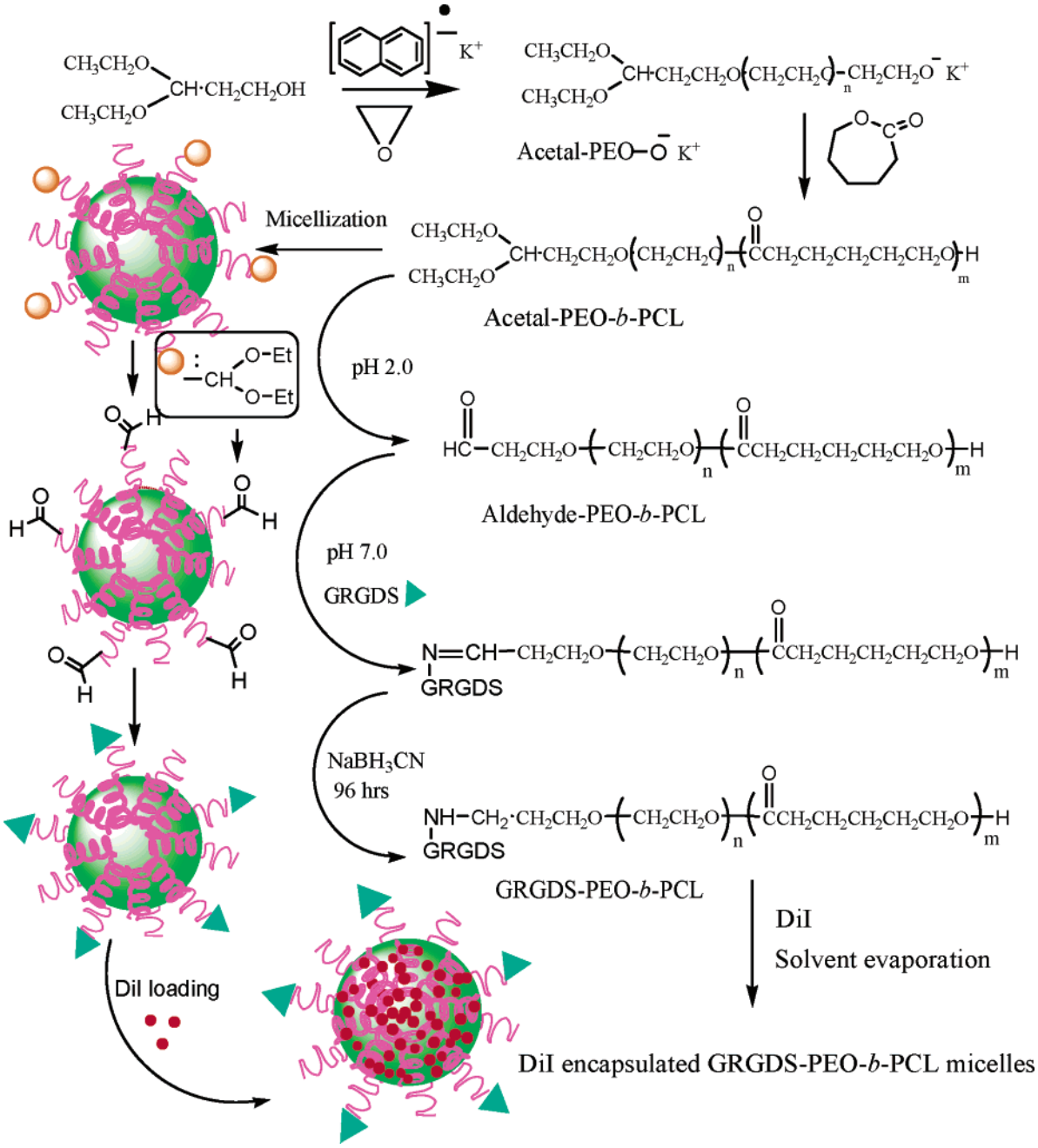

have low immunogenicity and avoid RES. Besides, peptides can easily be derivatized and engineered to achieve better in-vivo stability and tissue specificity.

In this manuscript, we report the development of poly(ethylene oxide)-*block*-poly(ϵ-caprolactone) (PEO-*b*-PCL) micelles decorated with a relatively small internalizing model peptide (e.g., GRGDS). Micelles of PEO-*b*-PCL have been extensively studied for the encapsulation of hydrophobic drugs and have proved to be a promising drug carrier for tumor targeting.[16−18] The results of previous research by our group and others indicate that PEO-*b*-PCL micellar delivery may reduce the internalization of hydrophobic drugs by various cells, however.[5,6] The arginine-glycine-aspartic acid (RGD) containing sequence is known to serve as a recognition motif in multiple ligands for integrins.[19,20] Integrins are a family of cell surface receptors which are responsible for anchoring cells to the extracellular matrix (ECM). Integrin-mediated cell attachment and internalization are exploited by a variety of viruses and bacteria for cell entry.[21,22] Various research groups also suggested that the RGD-containing peptides can be internalized by integrin-mediated endocytosis.[23−25] The small RGD molecule is as effective as its larger protein counterparts for supporting cell adhesion by attachment to integrin adhesion molecules, $\alpha_v\beta_3$ and $\alpha_v\beta_5$, which are overexpressed on activated endothelium and metastatic tumor cells. Besides, its simple, synthetic nature allows for straightforward chemistry for incorporation into biomaterials. Recently, the short RGD peptide has extensively been employed to facilitate attachment of cells in the field of tissue engineering, targeted drug or gene delivery.[26−33] In the present study, conjugation of RGD-containing peptides on PEO-*b*-PCL micellar surface was pursued to enhance the internalization of encapsulated molecules by target cells. On the basis of our results, a potential for RGD-modified micelles in enhancing the targeting efficacy of polymeric micellar delivery systems is envisioned.

Table 1. Characteristics of Polymers Prepared in This Study

polymer	PEO M_n[a] (g mol^{-1})	theoretical PCL M.wt (g mol^{-1})	PCL M_n[a] (g mol^{-1})	polymer M_n[b] (g mol^{-1})	polydispersity (M_w/M_n)[b]	PEO end group conjugation level (% M/M)
acetal-PEO	3600			3320	1.340	100[a]
acetal-PEO-*b*-PCL	3600	5000	1460	5160	1.458	100[a]
aldehyde-PEO-*b*-PCL	3600	5000	1380	4830	1.350	≥36.7[a]
GRGDS-PEO-*b*-PCL	3600	5000	1390	4910	1.467	50.0[c]
valine-PEO-*b*-PCL	3600	5000	1400	4930	1.307	N.D.[d]

[a] Determined by ^{1}H NMR. [b] Determined by GPC. [c] Determined by HPLC detection at 214 nm. [d] N.D.: not determined.

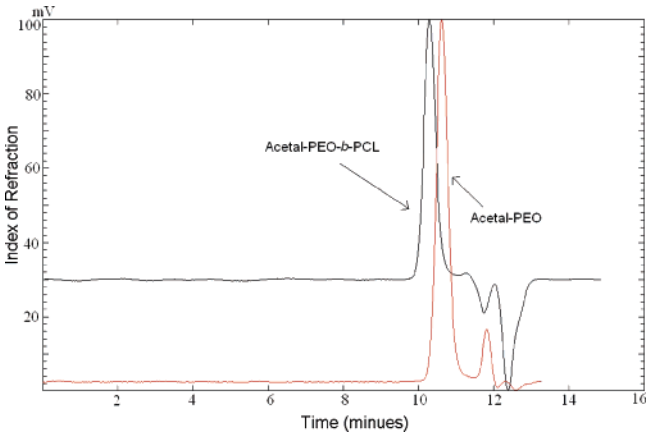

Figure 1. GPC chromatogram of acetal-PEO homopolymer and acetal-PEO-*b*-PCL block copolymer detected by refractive index detector (Model 410; Waters Inc.).

Materials and Methods

Materials. ϵ-Caprolactone (ϵ-CL) was purchased from Lancaster Synthesis, United Kingdom, was dried over calcium hydride at room temperature for 48 h, and was purified by vacuum distillation before use. Tetrahydrofuran (THF) was refluxed and distilled over sodium. Ethylene oxide (EO) was distilled twice, first in the presence of potassium hydroxide and second in the presence of calcium hydride. 3,3-Diethoxy-1-propanol (DEP), naphthalene, and potassium were bought from Sigma-Aldrich (St. Louis, MO) and were used as received. GRGDS was purchased from Bachem (Torrense, CA). Potassium naphthalene solution was prepared by conventional method[34] and the concentration was determined by titration. Cell culture media RPMI 1640, penicillin-streptomycin, fetal bovine serum, L-glutamine, and HEPES buffer solution (1 M) were purchased form GIBCO, Invitrogen Corp (United States). Fluorescent probes DiI and Alexa 488-concavalin A conjugate were purchased from Molecular Probes, United States.

Preparation and Characterization of Acetal-PEO-*b*-PCL Block Copolymers. Acetal-PEO-*b*-PCL was synthesized by a one-pot anionic ring opening polymerization at room temperature under argon stream adopting a previously reported method for the preparation of acetal-PEO-*b*-poly(D,L-lactide) (PEO-*b*-PDLLA) with some modifications (Scheme 1).[35] Briefly, 1 mmol (0.15 mL) of initiator (3,3-diethoxy-1-propanol) and 1 mmol (3.5 mL) of potassium naphthalene were added to 20 mL of dry THF. After 10 min of vigorous stirring, 114 mmol (5.7 mL) of condensed ethylene oxide (EO) was added via a cooled syringe to the mixture. The polymerization of EO proceeded for 2 days at room temperature under argon resulting in a highly viscous solution. A part of the reaction product was sampled to follow the progression of EO polymerization. Potassium naphthalene (about 0.1 mmol) was then added to stabilize the living chain end until the reaction solution turned pale green. To this solution, 42 mmol (20 mL THF solution) of ϵ-CL was introduced, and the mixture was stirred for 2 h. The copolymer was recovered by precipitation in ice-cold diethyl ether, by centrifugation (3000 rpm for 30 min), and by drying under vacuum at room temperature. The sample was stored at −20 °C.

Prepared polymers in each step were dissolved in $CDCl_3$ and were characterized by ^{1}H NMR (Bruker AM-300). Gel permeation chromatography (GPC) was also carried out to define the molecular weights and polydispersity of acetal-PEO and acetal-PEO-*b*-PCL. Briefly, 20 μL of polymer solution (20 mg/mL in THF) was manually injected into a 7.8 × 300 mm Styragel HMW 6E column (Waters Inc. Milford, MA), which was attached to an HP 1100 pump. The column was eluted with 1 mL/min THF. The elution pattern was detected at 35 °C by refractive index (Model 410; Waters Inc.) and dynamic light scattering detectors (PD 2000 DLS; Precision Detectors, Franklin, MA).

Preparation and Characterization of Aldehyde-PEO-*b*-PCL Micelles. Acetal-PEO-*b*-PCL copolymer was dissolved in acetone to provide a 20 mg/mL polymer concentration. The solution was then added dropwise to doubly distilled water under moderate stirring at 25 °C, followed by evaporation of acetone under vacuum. Average diameter and size distribution of the prepared micelles were measured by dynamic light scattering (DLS) using a Malvern Zetasizer 3000 (Malvern, United Kingdom) at a polymer concentration of 4 mg/mL. Conversion of acetal to aldehyde group under acidic condition was carried out on acetal-PEO-*b*-PCL micelles to protect PCL from hydrolysis under acidic condition.

The acetal groups on the surface of PEO-*b*-PCL micelles were converted to aldehyde groups by dropwise addition of 0.5 mol/L HCl at room temperature adjusting the pH of the medium to 2. After stirring for 2 h, the mixture was neutralized with NaOH (0.5 mol/L) to stop the reaction. The resulting micellar solution was first concentrated by ultracentrifugation with MILLIPORE Centrifugal Filter Device (Mw cutoff of 100 000 Da) then purified by a Sephadex G50 column using PBS (pH 7.0) as the eluent. Finally, the micellar solution was extensively dialyzed (molecular weight cut off of 3500 Da) against water to remove the salt and was freeze-dried for further use. Part of the freeze-dried sample was dissolved in $CDCl_3$ to obtain the ^{1}H NMR spectra.

Conjugation of GRGDS to Aldehyde-PEO-*b*-PCL Micelles. A sodium phosphate buffer (pH = 7.0, ionic strength 0.1 M) solution was added to aldehyde-PEO-*b*-PCL micelles to obtain 4 mg/mL polymer concentration. GRGDS was added and incubated with the polymeric micelles at 1:2 molar ratio (GRGDS:aldehyde-PEO-*b*-PCL) at room temperature under moderate stirring. After 2 h, $NaBH_3CN$ (10 equiv) was added to the polymer to reduce the Schiff base. After 4 days of reaction, the micellar solution was purified by a Sephadex G-50 column (Pharmacia Biotech, Germany) followed by dialysis against water (Mw cut off of 3000 Da). The resulting GRGDS-attached polymeric micelles were lyophilized and stored at −20 °C until use. Valine-conjugated PEO-*b*-PCL (valine-PEO-*b*-PCL) was also prepared by an identical protocol as the irrelevant ligand decorated micelles and was used as a control for the cell uptake studies.

The conjugation of peptide to micelles was first investigated by ^{1}H NMR spectroscopy in a qualitative manner. For this purpose, acetal-PEO-*b*-PCL, aldehyde-PEO-*b*-PCL, or GRGDS-PEO-*b*-PCL micellar solutions were prepared through addition of polymer solutions in acetone to D_2O as described above and used for ^{1}H NMR spectroscopy.

A gradient reverse high-performance liquid chromatography (HPLC) method was developed to quantify the density and conjugation efficiency of GRGDS on polymeric micelles. A μBondapak (Waters Corp., United States) C-18 analytical column (10 μm, 3.9 × 300 mm) was used. Gradient elution was performed at a flow rate of 1 mL/min (model 600 pump, Waters, Billerica, MA) with the mobile phases of 0.1% TFA in H_2O (solution A) and 0.1% TFA in 90/10 acetonitrile/H_2O (solution B). The mobile phase was programmed as follows: (1)

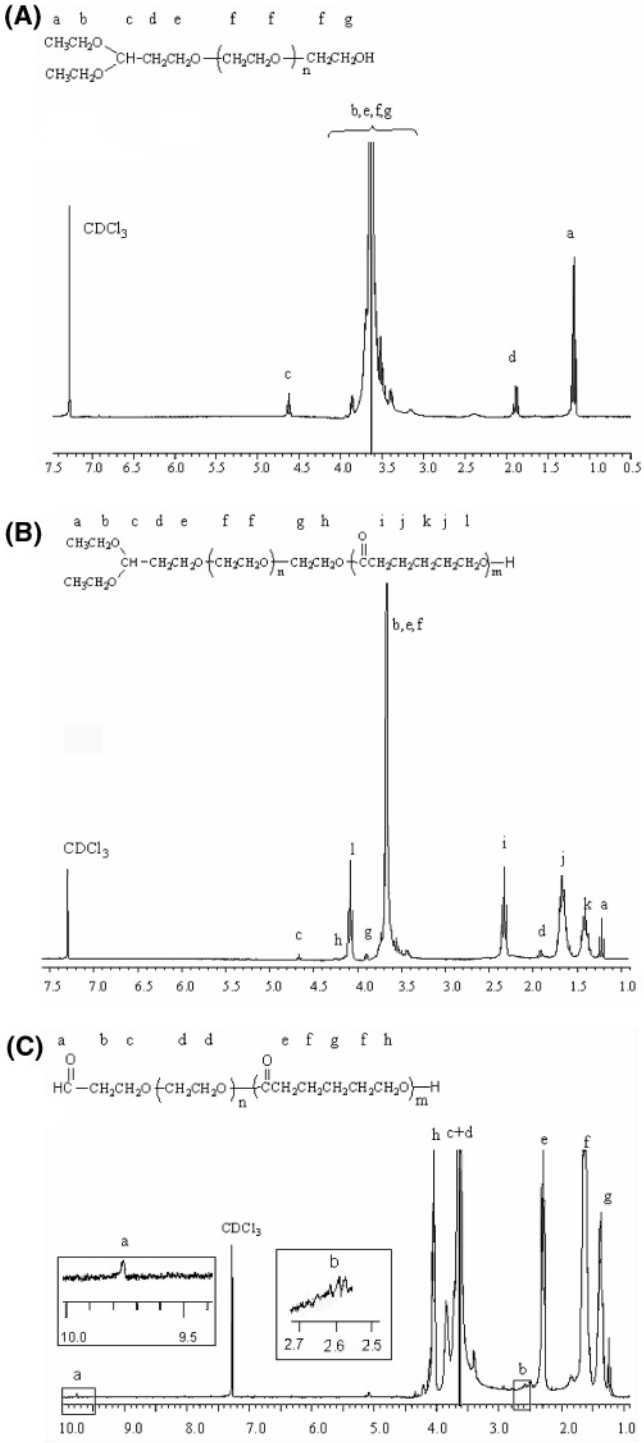

Figure 2. ^{1}H NMR spectrum of (A) acetal-PEO, (B) acetal-PEO-*b*-PCL, and (C) aldehyde-PEO-*b*-PCL in $CDCl_3$.

100% A for the first 1 min, (2) a linear gradient from 100% A to 60% A in 20 min, a linear gradient from 60% A to 0% A for 4 min, (4) 0% A for 2 min, (5) 0% A to 100% A in 4 min, and (6) 100% A for 5 min. GRGDS was incubated with either acetal or aldehyde-PEO-*b*-PCL micellar solution at a 1:2 molar ratio. The reaction mixture (20 μL) was directly injected into the system in duplicate at different time points after initiation of the reaction. Free peptide was detected with a Waters UV detector at 214 nm. The concentration of unreacted peptide in the reaction mixture was calculated on the basis of a calibration curve for peak areas at known concentrations of the peptide in phosphate buffer. The amount of conjugated peptide was then calculated by subtracting the amount of unreacted peptide from the amount of initial peptide added to the reaction and was expressed as the number of peptide molecules conjugated per 100 polymer chains.

Preparation and Characterization of DiI Loaded GRGDS- and Valine-PEO-*b*-PCL Micelles. Physical entrapment of hydrophobic fluorescent probe, DiI, was used to prepare fluorescent-labeled polymeric micelles for the cellular uptake investigations. DiI (10 μg/mL) and GRGDS-PEO-*b*-PCL copolymer (10 mg/mL) were dissolved in acetone (0.5 mL). This solution was added to 3 mL of water in a dropwise manner followed by evaporation of organic solvent under vacuum. The micellar solution was then centrifuged at 11 600 $\times$ *g* for 5 min to remove the DiI precipitates. An identical procedure was used for DiI loading in valine-PEO-*b*-PCL micelles. The hydrodynamic diameter of DiI-loaded micelles was measured by DLS as described above. An aliquot of the micellar solution was diluted with an equal volume of DMSO and was used to quantify the level of encapsulated DiI by UV−vis spectroscopy at 550 nm. The release of DiI from micelles was investigated in PBS containing lipid vesicles as the receiver phase as described previously.[6]

Cell Uptake Studies. Melanoma B16-F10 cells line was a generous gift from the laboratory of Dr. J. Samuel, University of Alberta. Cells were grown in RPMI 1640 complete growth medium supplemented with 10% fetal bovine serum, 1 w/v % L-glutamine, and 100 units/mL penicillin and 100 μg/mL streptomycin and were maintained at 37 °C with 5% CO_2 in a tissue culture incubator. Cells were seeded into a 24-well plate (1×10^5 cells/well) containing 1 mL of media to grow to ~70% confluence after 24 h incubation. Valine- or GRGDS-micelles containing DiI were then added and incubated with B16-F10 cells for 0, 0.5, 1, 3, 6, and 9 h at 37 or 4 °C. The final DiI and polymer concentration in each well was 0.5 μg/mL and 0.5 mg/mL, respectively. Incubation at 4 and 37 °C were used to differentiate between cell binding and internalization. Internalization is expected to be reduced at 4 °C since energy-dependent uptake is abolished at this temperature, whereas both receptor binding and internalization is expected to take place at 37 °C. Free DiI was dissolved in PBS with the aid of DMSO (<1%) and was incubated with cells for 3 h as positive control. Samples having free and encapsulated DiI without cells and cells incubated with the medium were used as negative controls. For the competition experiments, B16-F10 cells were preincubated with excess free GRGDS (1 mg/mL) for 30 min to saturate receptors and to inhibit the binding and internalization of GRGDS-conjugated micelles. Following the incubation period, medium was removed and cells were washed with cold PBS three times. Then, 1 mL of DMSO was added in each well to lyse cells. Fluorescence emission intensity of DiI at 565 nm (fluorescence concentration analyzer, Baxter, United States) provided means for the measurement of internalized DiI levels. DiI cellular accumulation was normalized with respect to total cellular protein content, which was quantified by Bradford method using bovine serum albumin (BSA) as standard. Percent uptake was calculated using the following equation[6]

$$\text{uptake (\%)} = \frac{\text{normalized concentration of internalized DiI}}{\text{concentration of encapsulated DiI added to each well}} \times 100$$

Confocal Microscopy Studies. The cell binding or internalization was also investigated using confocal fluorescent microscopy. B16-F10 cells were seeded into eight-well glass chamber slide (Lab-Tek, United States) containing RPMI complete growth media (1×10^5 cells/well). Following 12-h incubation at 37 °C, 20-μL aliquots of DiI loaded GRGDS- or valine-micelles were added to each well and were incubated with cells for 3 h at 37 or 4 °C. The final DiI and polymer concentrations were 0.6 μg/mL and 0.6 mg/mL, respectively. The medium was removed and cells were washed three times with cold PBS followed by fixing with 100 μL of 4% paraformaldehyde in PBS for 10 min. In competition experiments, excess free GRGDS (1 mg/mL) was added to the culture medium 30 min prior to the addition of DiI loaded micelles. After 1-h incubation at 37 °C, cells were washed three times with PBS, were treated with Alexa fluor 488-concavalin A for 10 min, and were fixed with 4% paraformaldehyde in PBS. The

fluorescent images of cells were analyzed using laser scanning confocal microscopy (Zeiss, LSM 510, Germany).

Results

Preparation and Characterization of PEO-*b*-PCL Micelles Bearing Functional Groups on Their PEO End. Acetal-PEO-*b*-PCL was synthesized by one-pot anionic ring polymerization (Scheme 1). Potassium alkoxide initiator can initiate the polymerization of EO without any side reaction to form heterotelechelic PEO having an acetal moiety at one end and a potassium alkoxide at the other end, which can initiate the anionic ring opening polymerization of cyclic lactones in turn.[35]

The GPC profile of acetal-PEO, sampled after the step of EO polymerization, and acetal PEO-*b*-PCL (Figure 1) was used to follow the progress of polymerization reaction and also to measure the number-average molecular weights and polydispersity of the prepared polymers. As expected, the GPC profile of acetal-PEO-*b*-PCL revealed an increase in its molecular weight compared to acetal-PEO, indicating the successful polymerization of ϵ-CL by acetal-PEO. The M_n of acetal-PEO and acetal-PEO-*b*-PCL was 3320 and 5160 g mol^{-1} and the polydispersity was 1.340 and 1.458, respectively (Table 1).

Figure 2A illustrates the ^{1}H NMR spectrum of acetal-PEO and related assignments. Comparing the intensity of methylene proton peaks for PEO (CH_2CH_2O, $\delta = 3.7$ ppm) to the intensity of peak of methyl protons for the acetal group (CH_3CH_2O, $\delta = 1.2$ ppm), the average M_n of the PEO was calculated to be 3600 g mol^{-1}. Figure 2B shows the ^{1}H NMR of acetal-PEO-*b*-PCL. Peaks contributed to acetal groups, that is, methyl protons of CH_3CH_2O, $\delta = 1.2$ ppm; methylene protons of $CHCH_2CH_2O$, $\delta = 1.9$ ppm; and methine protons $O-CH-CH_2$, $\delta = 4.6$ ppm were clearly observed in the ^{1}H NMR spectrum of acetal-PEO-*b*-PCL. The M_n of acetal-PEO-*b*-PCL calculated by comparing the peak intensity of methylene protons of PCL ($-CH_2-O$, $\delta = 4.1$ ppm) to that of PEO (CH_2CH_2O, $\delta = 3.7$ ppm) was 5060 g mol^{-1}. The number-average molecular weights measured by GPC were in good agreement with those measured by ^{1}H NMR but were usually lower than theoretical molecular weights calculated on the basis of the applied monomer/initiator ratios (Table 1).

In the next step, acetal-PEO-*b*-PCL assembled to polymeric micelles through a cosolvent evaporation method using acetone as the organic cosolvent. On the basis of DLS measurements, the average diameter and polydispersity index of prepared polymeric micelles were 76 nm and 0.02, respectively. The acetal groups on the surface of polymeric micelles were then transformed into aldehyde groups by acid treatment. Figure 2C shows the ^{1}H NMR spectrum of the produced block copolymer in $CDCl_3$. The intensity of peaks corresponding to the acetal group (methyl protons of CH_3CH_2O, $\delta = 1.2$ ppm and methine protons of $O-CH-CH_2$, $\delta = 4.6$ ppm) was reduced and the related peak for the aldehyde proton appeared at $\delta = 9.8$ ppm. The extent of conversion of acetal to aldehyde, estimated by ^{1}H NMR of the polymer by comparing the peak intensity of aldehyde proton (CHO, $\delta = 9.8$ ppm) to the PEO protons (CH_2CH_2O, $\delta = 3.7$ ppm) considering a PEO molecular weight of 3600 g mol^{-1}, was 36.7%.

Additional proof for the formation of acetal-PEO-*b*-PCL micelles and the conversion into aldehyde-PEO-*b*-PCL micelles in an acidic aqueous environment was obtained by ^{1}H NMR spectroscopy in D_2O (Figure 3A and 3B). Because of the limited mobility of the inner core of polymeric micelles in D_2O, the intensity of proton peaks originating from the core-forming

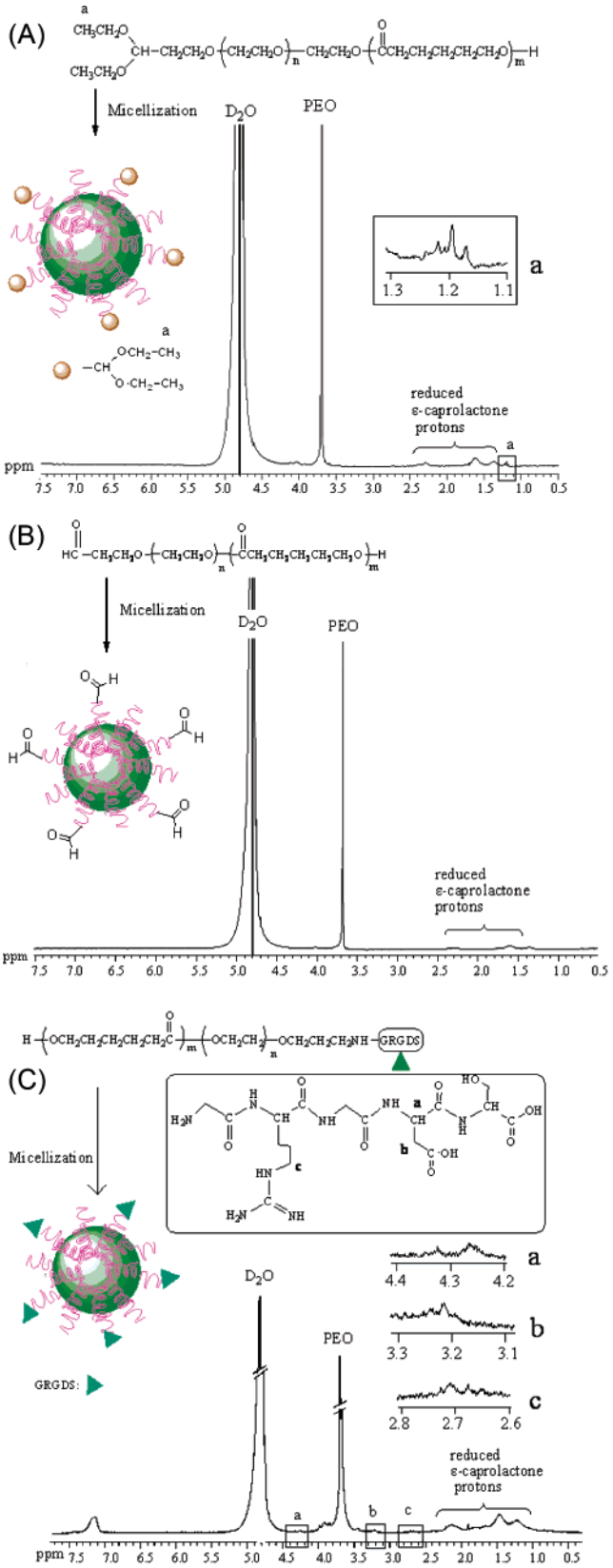

Figure 3. ^{1}H NMR spectrum of (A) acetal-PEO-*b*-PCL, (B) aldehyde-PEO-*b*-PCL, and (C) GRGDS-PEO-*b*-PCL micelles in D_2O.

block decreased dramatically compared with that in $CDCl_3$ where the formation of micelle is not expected. Small broad peaks at 1.2−2.0 ppm (Figure 3A and B) characteristic of the ϵ-caprolactone protons of the PCL segment for both acetal-PEO-*b*-PCL and aldehyde-PEO-*b*-PCL micelles show restricted

Table 2. Characteristics of DiI Loaded Polymeric Micelles Prepared in This Study

polymeric micelles	DiI/polymer loading ratio (w/w)	encapsulation efficiency (%)	micellar size ± SD (nm)	micellar polydispersity	DiI released after 12 h ± SD (%)
GRGDS-PEO-*b*-PCL	1:400	85.3 ± 2.4	76.7 ± 5.6	0.16	7.4 ± 1.6
valine-PEO-*b*-PCL	1:400	84.9 ± 1.9	74.8 ± 4.7	0.19	8.6 ± 1.2

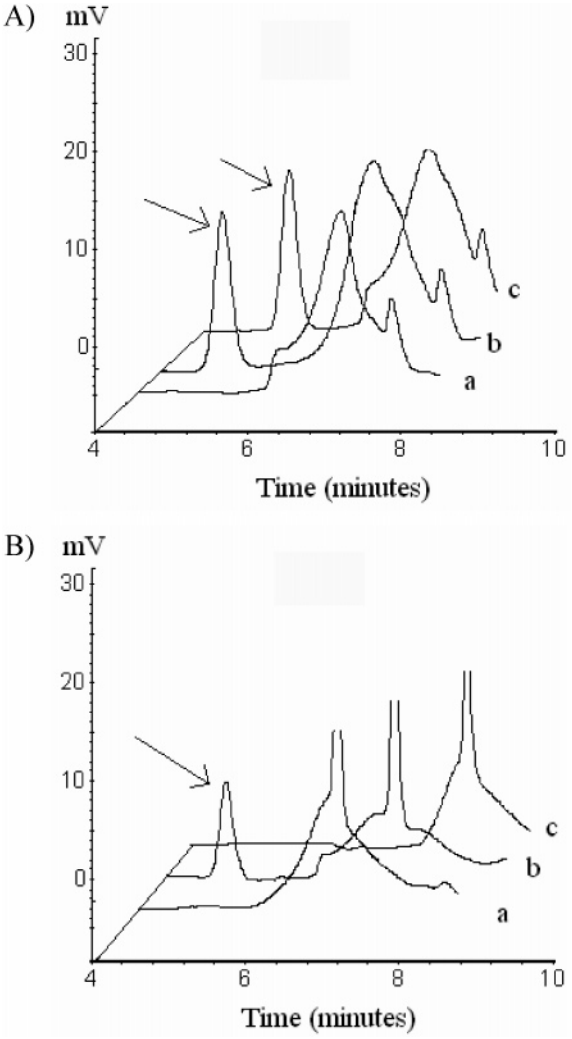

Figure 4. Reverse HPLC assessment of peptide conjugation to polymeric micelles. Unreacted GRGDS (arrowed peak) was eluted at 5.5 min. (A) Acetal-PEO-*b*-PCL micelles or (B) aldehyde-PEO-*b*-PCL micelles in PBS (pH = 7.0) were incubated with 0.1 mg/mL GRGDS for 2 h, followed by the addition of $NaBH_3CN$ and incubation for another 96 h. The reaction mixture (20 μL) was directly injected into the system at 1 and 72 h (b and c, respectively). Meanwhile, micelle solution in PBS without free GRGDS was also injected as the control (a).

motions of these protons compared to the ^{1}H NMR spectrum of the copolymers in $CDCl_3$ (Figure 2A and B). Peak corresponding to the acetal group (methyl protons of CH_3CH_2O, δ = 1.2 ppm) was observed with acetal-PEO-*b*-PCL micelles in D_2O (Figure 3A) but not with aldehyde-PEO-*b*-PCL micelles suggesting the ready conversion of acetal into aldehyde under acid treatment, although the peak corresponding to aldehyde proton was not observable in the ^{1}H NMR spectrum of aldehyde-PEO-*b*-PCL micelles in D_2O (Figure 3B).

Preparation and Characterization of GRGDS- and Valine-PEO-*b*-PCL Micelles. GRGDS and valine were conjugated separately at the PEO end of micelles through a reaction between the aldehyde group on the micelle with the terminal amino group of the peptide (or amino acid) at pH 7.0 (Scheme 1). The average diameters of prepared GRGDS-PEO-*b*-PCL and valine-PEO-*b*-PCL micelles were approximately 73 nm and the polydispersity indices were less than 0.20 on the basis of DLS analysis. In $CDCl_3$, peaks related to protons of GRGDS (δ = 2.7, 3.2, 4.3 ppm) were covered by PCL related peaks of PEO-*b*-PCL. For this reason, the ^{1}H NMR spectrum of GRGDS-PEO-*b*-PCL micelles was obtained in D_2O. GRGDS-PEO-*b*-PCL self-assembles to polymeric micelles in D_2O, where the intensity of the PCL related peaks will be quenched because of the rigidity of the micellar core. Under this condition, the PEO (δ = 3.7 ppm) and GRGDS proton (δ = 2.7, 3.2, 4.3 ppm) related peaks of GRGDS-PEO-*b*-PCL were readily observable (Figure 3C).

The HPLC chromatogram of the reaction mixture for acetal and aldehyde-PEO-*b*-PCL micelles is shown in Figure 4A and B, respectively. Free GRGDS was eluted at 5.4−6.2 min without any interference. With a set of GRGDS standard solution, the peak area was correlated with the injected peptide concentration (R^2 = 0.9998). No significant change in the peak area of free GRGDS after 1 and 72 h of incubation with acetal-PEO-*b*-PCL micelles was detected (Figure 4A). The 100% recovery of added GRGDS from a mixture of GRGDS and acetal-PEO-*b*-PCL micelles indicates the absence of GRGDS chemical conjugation, physical adsorption, or encapsulation by acetal-PEO-*b*-PCL micelles. In contrast, the peak area of GRGDS incubated with aldehyde-PEO-*b*-PCL micellar solution was significantly lower after 1-h reaction and completely disappeared after 72-h reaction (Figure 4B). Measurement of the concentration of free GRGDS remained after 72-h reaction revealed a 1:2 molar ratio for conjugated GRGDS:aldehyde-PEO-*b*-PCL at a molar peptide:polymer feed ratio of 1:2, corresponding to 100% conjugation efficiency.

Cell Binding and Uptake Studies. DiI was efficiently encapsulated in GRGDS- and valine-micelles reaching an encapsulation efficiency of >80% corresponding to a DiI/polymer w/w ratio of 0.25% for both systems. DiI was also slowly released from both micellar carriers. Within 12 h of incubation with lipid vesicles, GRGDS- and valine-micelles only released 7.4 and 8.6% of their DiI content, respectively (Table 2). The average diameter of DiI loaded GRGDS- and valine-micelles was 76.7 and 74.8 nm, respectively (Table 2).

Murine melanoma B16-F10 cells were incubated with DiI loaded GRGDS- or valine-micelles for various time periods at either 4 or 37 °C. The data pointed to a higher extent of cell binding as well as internalization for the GRGDS-modified micelles compared to valine-modified micelles (Figure 5). A rapid increase in the apparent uptake of DiI incorporated GRGDS- and valine-micelles (including membrane-bound and internalized) by melanoma cells during the first hour of incubation at 37 °C was observed. Uptake of encapsulated DiI proceeded at a lower rate for both systems within the next 8 h of incubation at 37 °C. A remarkable decrease in the association of both DiI loaded GRGDS- and valine-micelles with B16-F10 cells was observed at 4 °C. After 9 h of incubation at 37 °C, 5.75 and 3.33% of GRGDS- and valine-micelles were associated with cells, respectively. At 4 °C, 1.64 and 0.69% of GRGDS- and valine-micelles were associated with cells after 9 h of incubation, respectively.

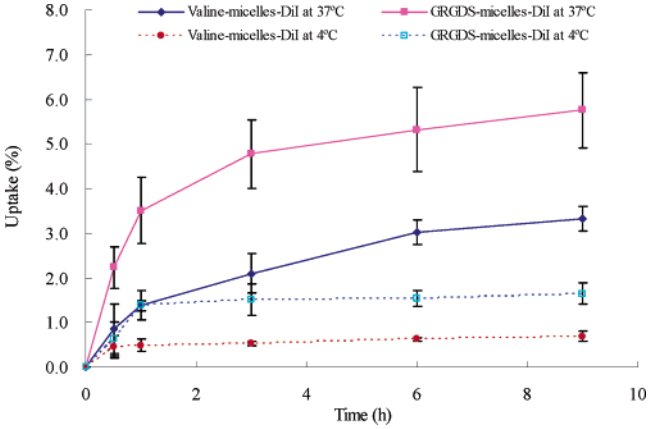

Figure 5. The rate of DiI loaded GRGDS- and valine-micelles uptake by B16-F10 cells at 37 or 4 °C. Each point represents average uptake % ± SD ($n = 4$).

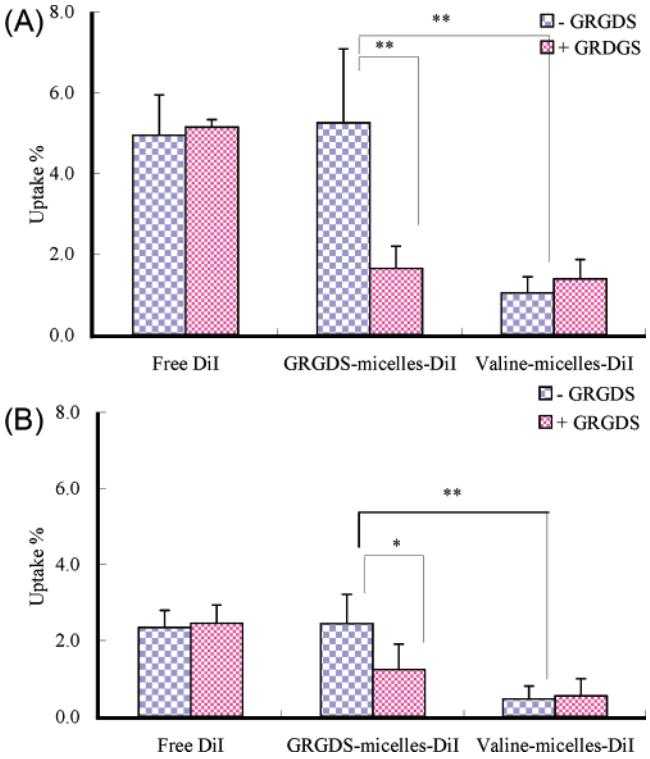

Figure 6. Cellular uptake of free DiI, DiI loaded GRGDS-micelles, and DiI loaded valine-micelles after 3 h of incubation at (A) 37 °C and (B) 4 °C with (+) or without (−) pretreatment with 10 mg/mL of free GRGDS. Each bar represents average uptake (%) ± SD ($n = 4$). *$P < 0.05$; **$P < 0.01$.

Competition with excess free GRGDS significantly inhibited the uptake of DiI loaded GRGDS-PEO-*b*-PCL micelles by 3.3-fold at 37 °C but did not affect the uptake of free DiI or DiI incorporated valine-PEO-*b*-PCL micelles (Figure 6). In the absence of free GRGDS peptide, GRGDS-modified micelles were able to increase the internalization of hydrophobic DiI by B16-F10 cells reaching to similar values to that of free hydrophobic DiI. Three hours after incubation of B16-F10 cells at 37 °C, 4.94, 5.25, and 1.03% cell association was observed for free DiI, DiI loaded GRGD, and valine-micelles, respectively. In the presence of free GRGDS, cell association was 5.14, 1.64, and 1.38% for the mentioned samples, respectively (Figure 6A). At 4 °C, the presence of free GRGDS resulted in a 2-fold decrease in the association of GRGDS-micelles with cells as well, but did not affect the cell association of free DiI or DiI-loaded valine-micelles. For free DiI, DiI incorporated GRGDS, and valine-polymeric micelles, percent cell uptake was 2.34, 2.44, and 0.46% in the absence of GRGDS, respectively. In the presence of competing peptide, cell association was 2.45, 1.23, and 0.54% for the same samples, respectively.

Internalization of DiI loaded polymeric micelles by melanoma cells was also investigated by confocal microscopy. Overall, the qualitative results from fluorescent microscopy studies were in good agreement with the quantitative results obtained from fluorescence spectroscopy, confirming the involvement of GRGDS-mediated internalization in the cellular uptake of GRGDS-micelles. After 3 h incubation at 37 or 4 °C, cells incubated with GRGDS-micelles (Figure 7A and C) showed remarkably more intense fluorescence in both cell membrane and cell cytoplasm than valine-micelles (Figure 7B and D), indicating facilitation of the cell binding and internalization for GRGDS-micelles. In addition, cells incubated with either GRGDS-micelles or valine-micelles at 37 °C (Figure 7A and B) demonstrated significantly stronger fluorescence both on cell membrane and, especially, in cytoplasm compared to samples incubated with cells at 4 °C (Figure 7C and D).

Figure 8 shows the cell binding and uptake of DiI loaded GRGDS-micelles in B16-F10 cells with or without free GRGDS pretreatment. Cells were incubated with DiI loaded GRGDS-micelles (red fluorescence, Figure 8A) and were stained with Alexa fluor 488-concavalin A (green fluorescence, Figure 8B). Superimposing two photographs (Figure 8A + B, 8E, and 8F) clearly displays the binding of DiI loaded GRGDS-PEO-*b*-PCL micelles to the cell membrane (arrows in Figure 8E and 8F) and their internalization in the cytoplasm. The yellow color is an indication for the coexistence of cell-related stain, that is, green fluorescence, and DiI, that is, red fluorescence, in the cell cytoplasm. Pretreatment of cells with free GRGDS, on the other hand, significantly inhibited the binding of GRGDS-micelles to B16-F10 cells leading to decreased intensity of yellow color, which indicates attenuated uptake of GRGDS-micelles into the tumor cells in the presence of free GRGDS (Figure 8C, 8D, 8C + D, and 8G).

Discussion

In this manuscript, we have reported the development of GRGDS decorated PEO-*b*-PCL micelles to enhance intracellular delivery of hydrophobic drugs to metastatic cancer cells. RGD-containing peptides are the specific ligands recognized by the cell surface receptor integrins and can lead to cell internalization. Overexpression of RGD binding receptors, that is, $\alpha_v\beta_3$ and $\alpha_v\beta_5$ integrins, on the endothelial cells of neovasculature in tumor and several invading/migrating cancer cells has been documented.[36−39] The B16-F10 murine cells are highly metastatic melanoma cells. The interaction between tumor cell and ECM is believed to contribute to the metastatic behavior of these tumor cells. Adhesive noncollagenous glycoproteins, such as laminin and fibronectin, serve pivotal roles in the basement membrane and stromal matrixes, respectively. The cell adhesive peptide GRGDS derived from the central cell-binding domain of fibronectin can competitively bind to the metastatic cells and can inhibit the cell binding to ECM, thus blocking the experimental metastasis of B16-F10 cells.[40,41] Another highly metastatic cell line B16-BL6, which expresses α_v integrins on the cell surface, was also employed to study the cell binding or metastasis inhibition, suggesting the integrin-mediated binding between cells and GRGDS.[39,42] Furthermore, various studies have suggested the involvement of RGD peptides in cellular

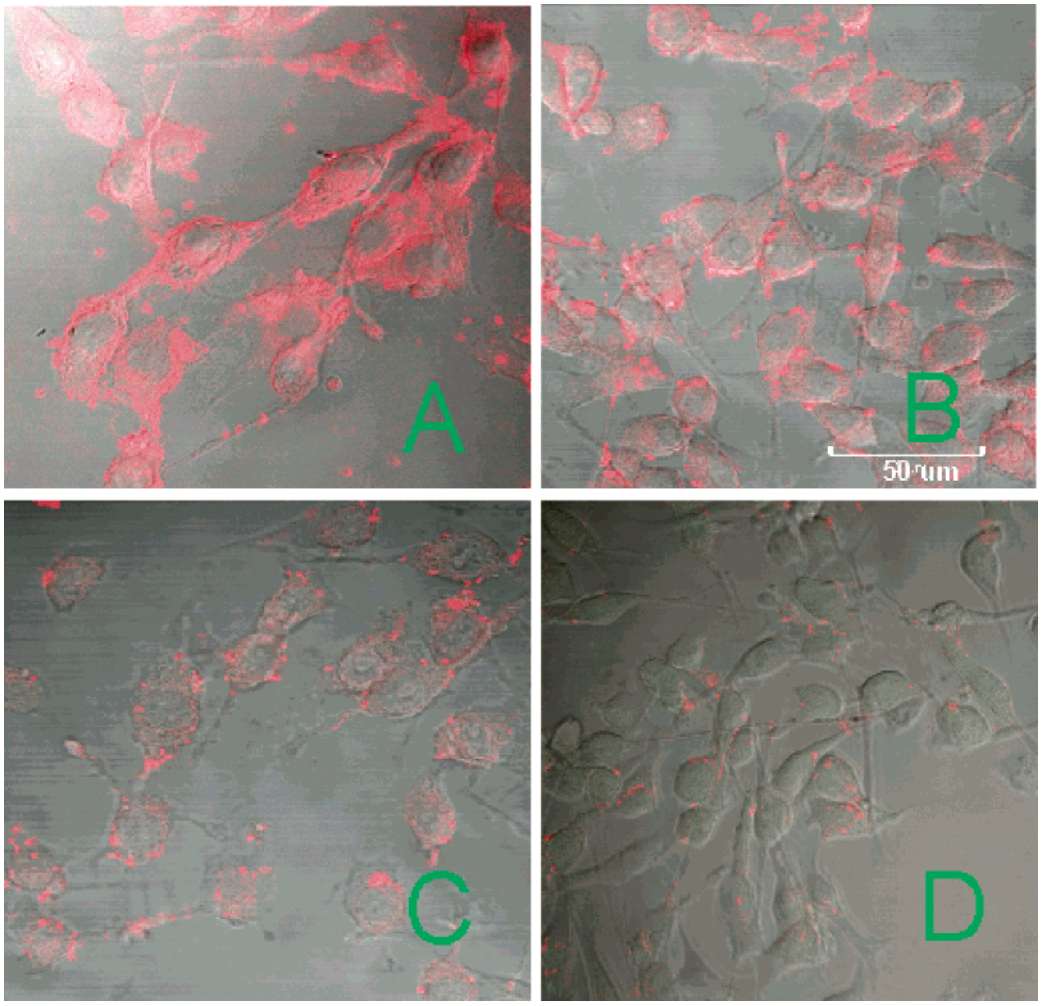

Figure 7. Confocal microscopy images of B16-F10 cells incubated with (A) DiI incorporated GRGDS-micelles at 37 °C, (B) DiI incorporated valine-micelles at 37 °C, (C) DiI incorporated GRGDS-micelles at 4 °C, and (D) DiI incorporated valine-micelles at 4 °C.

internalization through the integrin-mediated endocytosis,[10,24,43−46] pointing to the promising role for GRGDS-installed micelles in binding and internalization into metastatic melanoma B16 cancer cells.

To target tumor endothelial cells, Nasongkla et al. have developed PEO-*b*-PCL micellar system decorated with cyclic RGD-containing peptide (cRGDfK).[33] In that study, cRGDfK was conjugated to the PEO end of PEO-*b*-PCL micelles through a reaction between the free SH containing side groups on the thioacetyl-substituted cRGDfK and maleimide-PEO-*b*-PCL. In the present study, GRGDS-PEO-*b*-PCL micelles were developed through preparation of polymeric micelles bearing acetal groups on their surface, conversion of acetal to aldehyde under acidic condition, and further conjugation of the functionalized polymeric micelles with primary amine group of the GRGDS peptide by the Schiff base reaction at pH = 7.0 (Scheme 1, Figures 1 and 2). This method did not require any modification in the chemical structure of peptide, which is considered a primary advantage.

Conversion of acetal into aldehyde groups was carried out after formation of micelles from acetal-PEO-*b*-PCL for three reasons. First, acetal groups located at the distal end of the PEO block were more accessible when presented on micellar surface than those in random-coiled PEO strands. Second, aldol groups are prone to an aldol condensation in solution, thus reducing the yield of the subsequent coupling reaction. This phenomenon could be remarkably reduced in micellar solution, most probably because of the restricted motion of polymer chains that prevents the condensation of aldehyde groups. Finally, scission of the PCL segment during conversion of acetal to aldehyde under acidic condition is minimized in micellar form where the PCL segment in the hydrophobic micellar core is segregated from the aqueous environment. Similar molecular weights and polydispersity of the acetal, aldehyde, and peptide conjugates of PEO-*b*-PCL confirm the validity of this argument (Table 1), while the results of ^{1}H NMR spectroscopy in D_2O clearly indicated a core/shell structure for assemblies of acetal-, aldehyde-, and GRGDS-PEO-*b*-PCL block copolymers (Figure 3).

This synthesis method has been developed and used extensively by Nagasaki and co-workers to attach various ligands, such as monosaccharide derivatives and peptides, to the PEO-*b*-poly(lactide) micelles or to the PEO-PAMA micelles.[12,47,48] In those studies, a high functionality of aldehyde group for the PEO end (≥48%) and ligand conjugation (>20%) has been achieved. On the basis of our analysis, the GRGDS was completely consumed and conjugated at a density of 50% (one GRGDS molecule per two polymer chains) to the PEO end of polymeric micelles. The residual aldehyde groups is converted to hydroxyl groups by reduction with $NaBH_3CN$ as suggested in previous publications.[47]

It is not surprising that the GRGDS conjugation efficiency determined by HPLC is higher than the measured functionality (36.7%) of aldehyde group at the end of the PEO chains on the

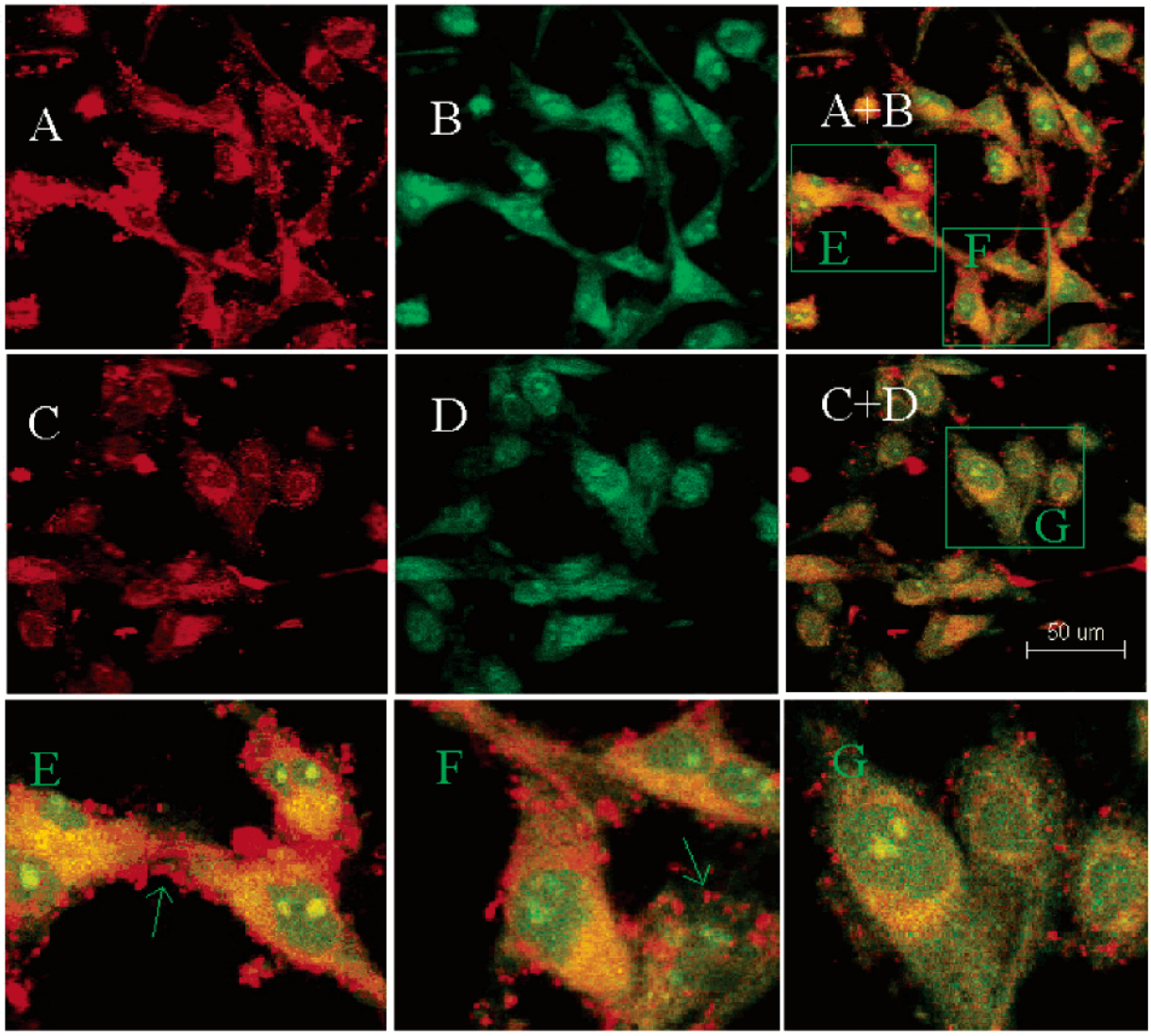

Figure 8. Fluorescence microscopic images show the blockage of the cellular internalization of GRGDS-micelles by free GRGDS. A, B, A + B, E, and F samples are prepared in the absence of free GRGDS. C, D, C + D, and G samples are pretreated with free GRGDS. (A) B16-F10 cells incubated with DiI loaded GRGDS-micelles (red fluorescence) for 1 h, (B) B16-F10 cells of slide A are stained with Alexa 488-concavalin A conjugate (green fluorescence), and (A + B) is prepared from superimposing A and B micrographs. (C) B16-F10 cells are treated with free GRGDS (10 mg/mL) for 30 min and then are incubated with DiI loaded GRGDS-micelles for 1 h, (D) B16-F10 cells of slide C are stained with Alexa 488-concavalin A conjugate (green fluorescence), and (C + D) is prepared from superimposing C and D micrographs. (E and F) Magnified regions from A + B slide. The yellow fluorescence shows the coexistence of green (cell stain) and red fluorescence (micelle stain) indicating the intracellular delivery of DiI by GRGD-micelles. Arrows indicate the cell membrane binding of GRGDS-micelles. (G) Magnified regions from C + D slide. The dominant green florescence in this sample (versus dominant yellow fluorescence in slides E and F) indicates the inhibition of GRGDS-micellar uptake by free GRGDS.

basis of ^{1}H NMR spectrum of aldehyde-PEO-*b*-PCL in $CDCl_3$. The aldehyde proton is not always readily detectable by ^{1}H NMR because of the keto−enol conversion and also because of the adol condensation.[13,35,47,49] This results in underestimation of the aldehyde density on the surface of polymeric micelles by ^{1}H NMR spectroscopy. The feed ratio of GRGDS to the polymer has a major effect on the conjugation efficiency obtained by this method, and the conjugation efficiency is expected to increase as the peptide to polymer feed ratio is enhanced.[47]

Valine was also conjugated to the surface of polymeric micelles as an irrelevant ligand for $\alpha_v\beta_3$ intergin with a similar polarity to that of GRGDS that can mimic the induced hydrophobicity by GRGDS on the surface of polymeric micelles. The prepared acetal-PEO-*b*-PCL, GRGDS-PEO-*b*-PCL, and valine-PEO-*b*-PCL micelles demonstrated very similar diameters of approximately 73 nm and unimodal distribution with polydispersity index less than 0.20 on the basis of DLS analysis, indicating that the conjugation of peptide or amino acid does not have any major effect on the micellar size and distribution.

A hydrophobic fluorescent probe, DiI, was used as a model molecule for encapsulation in polymeric micelles to study its cellular internalization. DiI was efficiently encapsulated by GRGDS- and valine-micelles and remained within the micellar carrier when incubated with lipid vesicles (Table 2). The inclusion of valine-polymeric micelles as a control in uptake studies was made to account for nonspecific endocytosis of polymeric micelles by tumor cells. In cell uptake studies, the free hydrophobic probe readily diffused into the melanoma cells. The high hydrophobic nature of the DiI is expected to ease its partition into the lipid membranes of the cancer cells leading to a greater extent of the cellular accumulation for free DiI. Encapsulation of DiI in valine-modified micelles, on the other hand, reduced its extent and rate of cellular internalization. A

similar observation for internalization of DiI loaded unmodified PEO-*b*-PCL micelles has been made previously with neuron cells and breast cancer cell lines.[6,50]

Conjugation of GRGDS on the surface of polymeric micelles, however, was shown to enhance the intracellular delivery of DiI to B16-F10 murine melanoma cells (Figure 5 and 7). Interestingly, the association of GRGDS-micelles was higher than valine-micelles even when incubated with melanoma cells at 4 °C, reflecting higher cell binding for GRGDS-micelles. A decrease in the cellular uptake (Figure 6) and binding was observed only for GRGDS-micelles in the presence of free peptide at both incubation temperatures (Figures 6 and 8). This points to the involvement of two possible mechanisms for cellular delivery of encapsulated hydrophobic probe by GRGDS modified micelles: (1) Enhanced internalization of DiI incorporated GRGDS modified micelles by receptor mediated endocytosis, which occurs predominantly at 37 °C, and (2) enhanced binding of the GRGDS modified micelles to cell integrins followed by diffusion of released DiI in the vicinity of the cell membrane into the cells which occurs at both incubation temperatures of 37 and 4 °C. In either case, the final outcome is enhanced intracellular delivery of encapsulated hydrophobic molecules to target cells. Finally, although conjugation of linear RGD-containing peptides like GRGDS to the surface of polymeric micelles is not expected to provide the required specificity for active tumor targeting after systemic administration, it may provide a viable tool for enhanced intracellular drug delivery to metastatic tumor cells through regional drug administration.

Conclusion

Synthetic methods based on acetal-terminated PEO-*b*-PCL are efficient and practical for introducing targeting peptide ligands on the surface of polymeric micelles. This study shows that modification of the polymeric micellar surface through conjugation of RGD-containing peptide ligands can enhance the intracellular delivery of hydrophobic drugs to metastatic tumor cells through integrin-mediated cell attachment and endocytosis. Conjugation of cell-specific peptide ligands to the hydrophilic shell of polymeric micelles may be pursued as a viable strategy to enhance the interaction of polymeric micellar carrier with specific cells, modulate micellar biodistribution, and increase the delivery encapsulated drug to its intracellular targets after systemic or regional routes of drug administration.

Acknowledgment. This study was supported by the Natural Sciences and Engineering Council of Canada (NSERC) (Grant No. G121210926). A.M. was supported by Rx and D HRF/CIHR graduate student research scholarship.

References and Notes

(1) Lavasanifar, A.; Samuel, J.; Kwon, G. S. *Adv. Drug Delivery Rev.* **2002**, *54*, 169−190.
(2) Yokoyama, M.; Okano, T. *Nippon Rinsho* **1998**, *56*, 3227−3234.
(3) Yokoyama, M.; Okano, T.; Sakurai, Y.; Fukushima, S.; Okamoto, K.; Kataoka, K. *J. Drug Targeting* **1999**, *7*, 171−186.
(4) Kwon, G.; Suwa, S.; Yokoyama, M.; Okano, T.; Sakurai, Y.; Kataoka, K. *J. Controlled Release* **1994**, *29*, 17−23.
(5) Allen, C.; Yu, Y.; Eisenberg, A.; Maysinger, D. *Biochim. Biophys. Acta* **1999**, *1421*, 32−38.
(6) Mahmud, A.; Lavasanifar, A. *Colloids Surf., B* **2005**, *45*, 82−89.
(7) Luo, L.; Tam, J.; Maysinger, D.; Eisenberg, A. *Bioconjugate Chem.* **2002**, *13*, 1259−1265.
(8) Sapra, P.; Allen, T. M. *Cancer Res.* **2002**, *62*, 7190−7194.
(9) Allen, T. M.; Sapra, P.; Moase, E.; Moreira, J.; Iden, D. *J. Liposome Res.* **2002**, *12*, 5−12.
(10) Xiong, X. B.; Huang, Y.; Lu, W. L.; Zhang, X.; Zhang, H.; Nagai, T.; Zhang, Q. *J. Controlled Release* **2005**, *107*, 262−275.
(11) Xiong, X. B.; Huang, Y.; Lu, W. L.; Zhang, H.; Zhang, X.; Zhang, Q. *Pharm. Res.* **2005**, *22*, 933−939.
(12) Nagasaki, Y.; Yasugi, K.; Yamamoto, Y.; Harada, A.; Kataoka, K. *Biomacromolecules* **2001**, *2*, 1067−1070.
(13) Jule, E.; Nagasaki, Y.; Kataoka, K. *Bioconjugate Chem.* **2003**, *14*, 177−186.
(14) Lee, E. S.; Na, K.; Bae, Y. H. *J. Controlled Release* **2003**, *91*, 103−113.
(15) Zeng, F.; Lee, H.; Allen, C. *Bioconjugate Chem.* **2006**, *17*, 399−409.
(16) Shuai, X. T.; Ai, H.; Nasongkla, N.; Kim, S.; Gao, J. M. *J. Controlled Release* **2004**, *98*, 415−426.
(17) Shenoy, D. B.; Amiji, M. M. *Int. J. Pharm.* **2005**, *293*, 261−270.
(18) Park, E. K.; Lee, S. B.; Lee, Y. M. *Biomaterials* **2005**, *26*, 1053−1061.
(19) Pasqualini, R.; Koivunen, E.; Ruoslahti, E. *Braz. J. Med Biol. Res.* **1996**, *29*, 1151−1158.
(20) Ruoslahti, E. *Annu. Rev. Cell Dev. Biol.* **1996**, *12*, 697−715.
(21) Isberg, R. R.; Van Nhieu, G. T. *Trends Cell Biol.* **1995**, *5*, 120−124.
(22) Logan, D.; Abu-Ghazaleh, R.; Blakemore, W.; Curry, S.; Jackson, T.; King, A.; Lea, S.; Lewis, R.; Newman, J.; Parry, N.; Rowlands, D.; Stuart, D.; Fry, E. *Nature* **1993**, *362*, (6420), 566−568.
(23) Ivanenkov, V. V.; Menon, A. G. *Biochem. Biophys. Res. Commun.* **2000**, *276*, 251−257.
(24) Temming, K.; Schiffelers, R. M.; Molema, G.; Kok, R. J. *Drug Resist. Update* **2005**, *8*, 381−402.
(25) Chen, Y.; Xu, X.; Hong, S.; Chen, J.; Liu, N.; Underhill, C. B.; Creswell, K.; Zhang, L. *Cancer Res.* **2001**, *61*, 2434−2438.
(26) Smith, E.; Yang, J.; McGann, L.; Sebald, W.; Uludag, H. *Biomaterials* **2005**, *26*, 7329−7338.
(27) Kim, W. J.; Yockman, J. W.; Lee, M.; Jeong, J. H.; Kim, Y. H.; Kim, S. W. *J. Controlled Release* **2005**, *106*, 224−234.
(28) Harvie, P.; Dutzar, B.; Galbraith, T.; Cudmore, S.; O'Mahony, D.; Anklesaria, P.; Paul, R. *J. Liposome Res.* **2003**, *13*, 231−247.
(29) Kunath, K.; Merdan, T.; Hegener, O.; Haberlein, H.; Kissel, T. *J. Gene Med.* **2003**, *5*, 588−599.
(30) Chen, X.; Plasencia, C.; Hou, Y.; Neamati, N. *J. Med. Chem.* **2005**, *48*, 1098−1106.
(31) Bibby, D. C.; Talmadge, J. E.; Dalal, M. K.; Kurz, S. G.; Chytil, K. M.; Barry, S. E.; Shand, D. G.; Steiert, M. *Int. J. Pharm.* **2005**, *293*, 281−290.
(32) Smith, E.; Bai, J.; Oxenford, C.; Yang, J.; Somayaji, R.; Uludag, H. *J. Polym. Sci., Part A: Polym. Chem.* **2003**, *41*, 3989−4000.
(33) Nasongkla, N.; Shuai, X.; Ai, H.; Weinberg, B. D.; Pink, J.; Boothman, D. A.; Gao, J. *Angew. Chem., Int. Ed.* **2004**, *43*, 6323−6327.
(34) Scott, N. D.; Walker, J. F.; Hansley, V. L. *J. Am. Chem. Soc.* **1936**, *58*, 2442−2444.
(35) Scholz, C.; Iijima, M.; Nagasaki, Y.; Kataoka, K. *Macromolecules* **1995**, *28*, 7295−7297.
(36) Brooks, P. C.; Clark, R. A.; Cheresh, D. A. *Science* **1994**, *264*, 569−571.
(37) Varner, J. A.; Cheresh, D. A. *Curr. Opin. Cell Biol.* **1996**, *8*, 724−730.
(38) Albelda, S. M.; Mette, S. A.; Elder, D. E.; Stewart, R.; Damjanovich, L.; Herlyn, M.; Buck, C. A. *Cancer Res.* **1990**, *50*, 6757−6764.
(39) Katagiri, Y. U.; Murakami, M.; Mori, K.; Iizuka, J.; Hara, T.; Tanaka, K.; Jia, W. Y.; Chambers, A. F.; Uede, T. *J. Cell. Biochem.* **1996**, *62*, 123−131.
(40) Humphries, M. J.; Yasuda, Y.; Olden, K.; Yamada, K. M. *Ciba Found. Symp.* **1988**, *141*, 75−93.
(41) Humphries, M. J.; Yamada, K. M.; Olden, K. *J. Clin. Invest.* **1988**, *81*, 782−790.
(42) Oku, N.; Tokudome, Y.; Koike, C.; Nishikawa, N.; Mori, H.; Saiki, I.; Okada, S. *Life Sci.* **1996**, *58*, 2263−2270.
(43) Shayakhmetov, D. M.; Eberly, A. M.; Li, Z. Y.; Lieber, A. *J. Virol.* **2005**, *79*, 1053−1061.

(44) Wencel-Drake, J. D.; Frelinger, A. L., III; Dieter, M. G.; Lam, S. C. *Blood* **1993**, *81*, 62−69.
(45) Xiong, X. B.; Huang, Y.; Lu, W. L.; Zhang, X.; Zhang, H.; Nagai, T.; Zhang, Q. *J. Pharm. Sci.* **2005**, *94*, 1782−1793.
(46) Harbottle, R. P.; Cooper, R. G.; Hart, S. L.; Ladhoff, A.; McKay, T.; Knight, A. M.; Wagner, E.; Miller, A. D.; Coutelle, C. *Hum. Gene Ther.* **1998**, *9*, 1037−1047.
(47) Yamamoto, Y.; Nagasaki, Y.; Kato, M.; Kataoka, K. *Colloids Surf., B* **1999**, *16*, 135−146.
(48) Wakebayashi, D.; Nishiyama, N.; Yamasaki, Y.; Itaka, K.; Kanayama, N.; Harada, A.; Nagasaki, Y.; Kataoka, K. *J. Controlled Release* **2004**, *95*, 653−664.
(49) Iijima, M.; Nagasaki, Y.; Okada, T.; Kato, M.; Kataoka, K. *Macromolecules* **1999**, *32*, 1140−1146.
(50) Maysinger, D.; Berezovska, O.; Savic, R.; Soo, P. L.; Eisenberg, A. *Biochim. Biophys. Acta* **2001**, *1539*, 205−217.

BM060967G